



Autoignition Modes in a Shockless Explosion Combustor

Fatma Cansu Yücel¹(✉), Fabian Habicht¹, Myles Bohon²,
and Christian Oliver Paschereit¹

¹ Chair of Fluid Dynamics, Technische Universität Berlin,
Straße des 17. Juni 135, 10623 Berlin, Germany
f.yuecel@tu-berlin.de

² Chair of Pressure Gain Combustion, Technische Universität Berlin,
Straße des 17. Juni 135, 10623 Berlin, Germany

Abstract. Pressure gain combustion as an alternative to isobaric combustion has been in the focus of research for the past decades as it potentially allows for increasing the thermal efficiency of conventional gas turbines significantly. Beside the most known concepts, such as pulse detonation and rotation detonation combustors, the shockless explosion combustor (SEC) has been proposed. In contrast to the previously mentioned detonation-based concepts the SEC process is based on a thermal explosion, hence avoiding entropy generation caused by propagating detonation waves. Conceptually, this is achieved through a homogeneous autoignition of the fuel–oxidizer mixture, which is realized by the proper stratification of the fuel concentration throughout the combustor, leading to a gradual rise in pressure. Since the process of autoignition is highly sensitive to perturbations, local deviations in the initial state of the mixture lead to a variety of autoignition modes. In this work, an SEC test rig is used to investigate the impact of different fuel injection profiles on the formation of autoignition modes. Pressure transducers are used to measure the pressure rise subsequent to the autoignition event. *k*-means clustering is applied to a set of pressure data to classify the measured pressure profiles. The same method was used to cluster the respective injection profiles. The results reveal that the gradient in reactivity is of major importance and can be used for increasing the pressure rise through ignition.

Keywords: Pressure gain combustion · Modes of autoignition · *k*-means clustering

1 Introduction

Implementing pressure gain combustion into a conventional gas turbine is a promising concept for increasing the overall thermal efficiency of the thermodynamic cycle. One concept among others is the shockless explosion combustor (SEC), which has been studied numerically and experimentally in previous works [1, 2, 6, 8]. The concept is based on a periodic combustion process (Fig. 1),

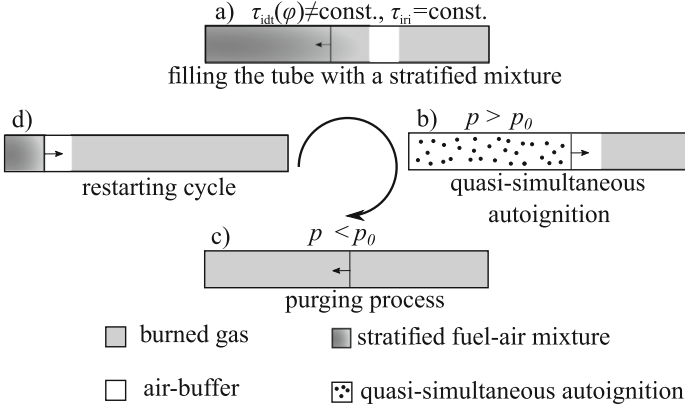


Fig. 1. Sketch of the SEC cycle.

including the quasi-instantaneous autoignition of a previously injected fuel–air package. The combustor is fed with a continuous air flow in which a well-defined fuel profile is added resulting in an axially stratified fuel–air mixture (Fig. 1a). The injected fuel profile has been tailored in order to compensate for the variation in residence time such that a simultaneous ignition of the entire combustor volume is achieved (Fig. 1b). Subsequent to the combustion event a pressure wave is induced that travels downstream. At the acoustically open outlet of the combustor the pressure wave is reflected as an expansion wave (Fig. 1c). The expansion wave then travels upstream and induces a pressure drop at the combustor inlet, which supports the refilling process (Fig. 1d).

The amplitude of the pressure rise induced by the ignition depends on the ignition homogeneity [8]. In particular, a perfectly homogeneous autoignition, is associated with a maximum rise in pressure. Since the ignition delay time τ_{idt} is a function of the local temperature T , pressure p and equivalence ratio φ the ignition time relative to the start of the injection τ_{iri} can be well controlled by the proper adjustment of the local equivalence ratio when assuming T and p to remain constant. However, a perfectly homogeneous autoignition is not feasible in applications and thus regarded as more of a theoretical consideration. In experiments, small but unavoidable perturbations in the injection process (e.g. pressure, temperature, and mixture composition) lead to deviations in the local ignition time τ_{iri} . The resulting spatial gradient in τ_{iri} causes an autoignition front, propagating with the velocity u_{ai} away from an exothermic center (region with increased reactivity). The propagating reaction front can be classified in four regimes that were first identified by Zel’dovich [11]. Based on his observations Zel’dovich introduced a dimensionless parameter:

$$\xi = \frac{a}{u_{\text{ai}}} \quad (1)$$

with the speed of sound a . Gu et al. defined lower and upper limits of ξ , ξ_l and ξ_u , respectively. Based on these limits the occurrence of different modes can be summarized as follows [4,5]:

$\xi > \xi_u$:	subsonic autoignitive flame propagation or deflagration,
$\xi_l < \xi < \xi_u$:	coupling of a reaction front with a pressure wave forming a detonation,
$0 < \xi < \xi_l$:	supersonic autoignitive flame propagation,
$\xi = 0$:	thermal explosion (homogeneous autoignition).

Despite the unavoidable cycle-to-cycle variation in the local ignition time in the application, an overall increase in the pressure amplitude was achieved in a previous study [10] by applying a closed-loop control of the fuel injection based on the cycle-averaged pressure rise. However, a significant cycle-to-cycle variation in the recorded pressure rise remained. Measurements with an optically accessible combustor were conducted to examine single ignition events to further analyze the underlying effects. The results revealed the formation of different autoignition modes to be responsible for the cycle-to-cycle variation.

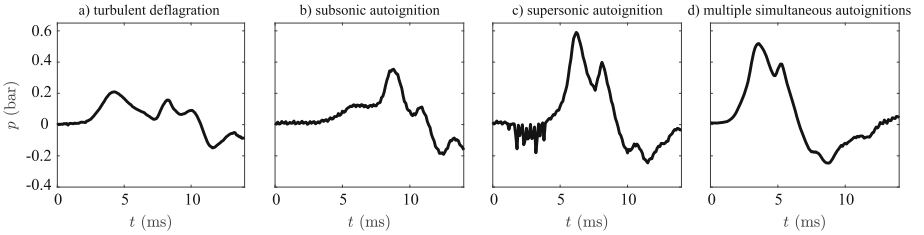


Fig. 2. Pressure histories of different autoignition modes observed by optical measurements in combination with pressure measurements in [10].

Four different autoignition modes were identified in [10] based on optical measurements in combination with pressure records: a) turbulent deflagration, b) subsonic autoignition, c) supersonic autoignition and d) aerodynamic confinement by multiple simultaneous autoignition fronts. Figure 2 shows example pressure histories for each case. It was observed that the simultaneous initiation of multiple autoignitions can lead to a similar rise in pressure compared with a supersonic autoignition. However, the differentiation between these two modes requires optical measurement and cannot be identified based on pressure data exclusively since the rise in pressure appears similar in both cases. Moreover, it was observed that the ignition characteristics of the applied fuel impacted the autoignition process. The used fuel dimethyl-ether (DME), as most hydrocarbon fuels, exhibits a negative temperature coefficient, meaning within a certain temperature range the ignition delay time decreases with an increasing temperature leading to a multi-stage ignition behaviour [7]. Single-stage ignitions are

accompanied by a fast and quasi-instantaneous heat release, whereas multi-stage ignition processes are characterized by a temporally distributed heat release during each stage. An increasing heat release contributes to a faster propagating autoignition front, and thus, leading to a greater aerodynamic confinement. Consistently, a two-stage ignition was found in the experiments to correlate with a lower rise in pressure (Fig. 2b) while a single-stage ignition was associated with a higher pressure rise (Fig. 2c and d).

Taking these observations as a basis, in this work, the formation of autoignition modes as a consequence of the fuel concentration distribution is evaluated based on pressure measurements. Therefore, a set of pressure data is evaluated by applying a clustering algorithm allowing for the identification of characteristic pressure histories, which are subsequently correlated to the fuel concentration distribution inside the combustor. The probability of appearance of the different ignition modes is determined with respect to the applied fuel injection profile.

2 Experimental Setup and Measurement Procedure

A test rig was designed to allow for the investigation of the autoignition process in stratified mixtures under atmospheric pressure and high temperature conditions. A cross section of the used test facility is sketched in Fig. 3. An air preheater is applied upstream of the fuel injection station in order to rise the air temperature up to 1023 K. A restriction downstream of the preheater is implemented to prevent pressure waves that occur subsequent to the ignition from propagating upstream. DME is used as fuel due to its short ignition delay times at the applied temperatures and atmospheric pressure conditions [3]. This enables the examination of the autoignition process in the combustor section. The fuel is guided through a vaporizer in order to ensure gaseous injection and is subsequently injected downstream of the restriction into the air flow by ten circumferentially distributed ports, each individually controlled by a high-speed solenoid valve (Staiger VA 204-716). Adjusting the number of open valves allows for a precise injection of a pre-defined fuel trajectory within a given injection period t_{inj} . The feeding line pressure is controlled by applying a high-speed dome-loaded pressure regulator (Swagelok RD6) which prevents a pressure drop during the fuel injection duration. A convection tube with a length of 500 mm and an inner diameter of 40 mm is mounted between the injection station and the combustor to compensate for the ignition delay time, which ensures the ignition event to take place inside the combustor section. The combustor consists of a 500 mm stainless steel tube equipped with four high-speed, piezoresistive, pressure transducers P1 to P4 (Kulite EWCTV-312), as shown in Fig. 3. Two low-speed, thin-film metal, static pressure transducers FA and FF (Festo SPTW) are installed to monitor the air and fuel supply pressures, respectively. Thermocouples T1 and T2 record the wall temperature during each run.

Different injection trajectories are defined by the simultaneous operation of a number of valves. By this, a defined fuel profile is injected into a continuous air flow with a frequency of 5 Hz. The local equivalence ratio is varied between

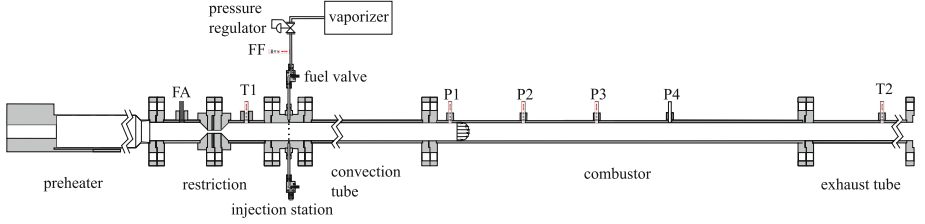


Fig. 3. Sketch of the atmospheric test rig equipped with high frequency pressure transducers (P1–P4), thermocouples (T1–T2) and low frequency pressure transducers (FF and FA).

$\varphi \in [1, 1.6]$ by adjusting the number of simultaneously open valves during the injection. The air mass flow rate was set to a steady-state value of 30 kg/h resulting in a mean air flow velocity of 18.5 m/s for the given boundary conditions. At the beginning of each cycle a defined mixture profile is added to the continuous air flow for a total injection duration of $t_{inj} = 30$ ms. Each injection trajectory is defined by ten individual valve settings each operated for 3 ms. The average number of open valves is restricted to a range between 7 and 7.8, ensuring a comparable fuel mass flow rate in each cycle with a maximum deviation of 10% in the global equivalence ratio. Pressure data are recorded subsequent to ignition of 40 individual cycles with a sampling frequency of 10 kHz.

2.1 *k*-means Clustering

A total number of 1080 cycles from measurements with 27 arbitrary injection trajectories were examined. The pressure signal at sensor P2 (see Fig. 3) was evaluated for each individual cycle for $50 \text{ ms} \leq t \leq 150 \text{ ms}$. The recorded pressure signals were classified using *k*-means clustering. The iterative algorithm starts with a number of *k* cluster centers $C_{k,i}$, which are initiated from randomly chosen pressure traces. Each cycle data is then assigned to the nearest cluster center based on the euclidean distance

$$d(p_j, C_{k,i}) = \|p_j - C_{k,i}\|_2, \quad (2)$$

where p_j denotes the pressure signal of cycle *j*. Subsequently, the cluster centers are recalculated from the cycle-averaged pressure signals from all cycles that are associated to the respective clusters. By iterating this procedure until the assignment of the pressure signals does not change anymore, an optimum classification is found. The results are characterized by the sum of distances to the cluster centers, according to

$$D_k = \sum_{i=1}^k \sum_{j=1}^{N_i} d(p_j, C_{k,i}), \quad (3)$$

where N_i denotes the number of cycles that are assigned to the cluster *i*. For convenience in the discussion the individual clusters for pressure traces are given

roman numeral designations and clusters for fuel profiles are given alphabetic designations. However, the solution only represents a local optimum as the result depends on the random choice of initial cluster centers. Therefore, the algorithm is executed independently for 50 times and the solution with the minimum value of D_k is chosen, as it most likely represents the global optimum. In order to evaluate the quality of the clustering, the maximum correlation coefficient R_{\max} between two individual cluster centers is calculated:

$$R_{\max} = \max(R(p_i, p_j)) \quad , \quad i, j = 1 \dots k. \quad (4)$$

In this work, the value of R_{\max} is used to identify a reasonable k to ensure fundamentally different clusters with minimum resemblance, while minimizing the variation within each cluster.

2.2 Fuel Injection Modelling

To ensure a precise stratification of the injected fuel profile, previous investigations on the applied injection strategy have been conducted. The results clearly demonstrate the ability to inject a stratified mixture within the injection duration, which remains preserved during convection until the onset of ignition. Detailed results can be found in [9]. However, a summary is provided in the following for the sake of completeness. In general, the measurements revealed that by adjusting the number of open valves the fuel concentration distribution inside the combustor can be controlled. It was found that the preservation of the fuel profile is independent of the temperature and mainly dependent on the spatial width $\chi = \bar{u}_{\text{air}} t_{\text{inj}}$ of the injected profile, where \bar{u}_{air} is the mean air flow velocity and t_{inj} is the injection duration.

Further investigations were conducted in [10] at varying temperatures of the air flow. The volumetric flow rate was kept constant allowing for a quantification of the impact of the Reynolds number on the diffusion processes. By this, the impact of turbulent fluctuations on the preservation of the injected fuel profile was analyzed. Based on the measurement data a simulation tool was developed solving the one-dimensional diffusion equation. Figure 4a illustrates an example injection trajectory (black line) with a duration of 30 ms assembled from ten consecutive valve settings. Since the injection in the experiments is affected by the inertia of the valves a polynomial Bézier curve was used to model the gradual change in the injected fuel flow rate. Moreover, the initial opening speed and the time of the valves are used as parameters for the adjustment of the valve behavior. The parameters were determined by matching the measured concentration profiles with the calculation results for a number of generic injection trajectories. The obtained model parameters were subsequently used to assess the fuel concentration at the injection station for arbitrary injection trajectories (red line).

Comparing the measurement data with the simulation results (Fig. 4b) revealed that the fuel distribution inside the combustor can be very well reproduced by the one-dimensional calculations. Hence, the fuel concentration distribution before the onset of ignition can be accurately predicted.

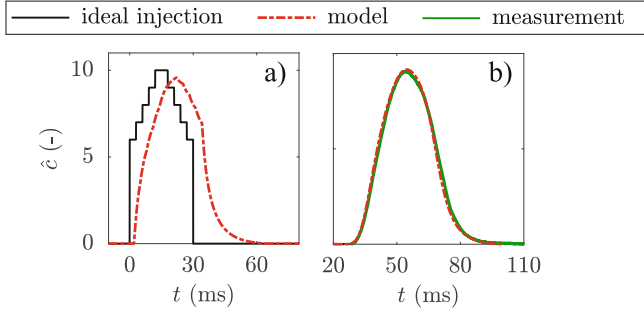


Fig. 4. Actual and modeled fuel injection trajectory (a), measured and modeled fuel concentration profile (b).

3 Results

In this section, first, all pressure signals will be clustered using the previously introduced k -means algorithm. Next, the one-dimensional simulation tool will be used to calculate the fuel distribution before the onset of ignition. The obtained fuel profiles are then clustered likewise and subsequently correlated to the obtained pressure clusters.

3.1 Clustering the Pressure Signals

Figure 5 shows the different cluster centers $C_{k,i}$ (red lines) obtained for $k = 2, 3$ and 4. The clusters are sorted in ascending order based on the maximum pressure amplitude. This parameter is chosen since it is a driving parameter in the performance of the SEC. Further, it has been proven to be a suitable control parameter for an optimization approach of the SEC process [10]. The gray lines visualize the individual pressure traces of cycles that are assigned to the respective cluster. The number of cycles that are assigned to a certain cluster is noted on top of each figure. As expected, an increasing k leads to a higher congruence of the associated pressure traces. However, comparing the clusters obtained for $k = 3$ with the autoignition modes presented in Fig. 2, a great correspondence of the respective clusters and modes is visible. Cluster $C_{3,I}$ shows features which have been observed for turbulent flames, while $C_{3,II}$ show great correspondence with a two-stage ignition, inducing a faster propagation autoignition front. $C_{3,III}$ exhibits similar features as a single-stage autoignition, which is associated with a high increase in pressure and a supersonic autoignition front.

When comparing the clusters obtained for each k , it is apparent that an increasing k results in a greater resemblance of some of the obtained clusters. While all clusters obtained for $k = 2$ and $k = 3$ seem fundamentally different, $C_{4,I}$ and $C_{4,II}$ show notable similarities. However, in order to objectively determine a reasonable k , a cross-correlation of the clusters obtained for each k is calculated

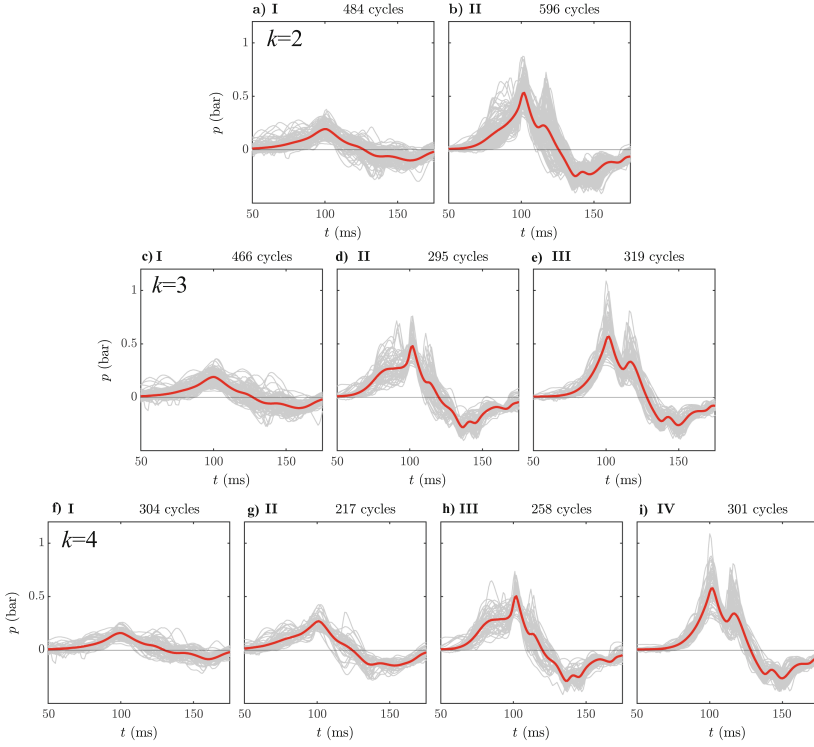


Fig. 5. Result of the k -means algorithm for $k = 2, 3$ and 4 .

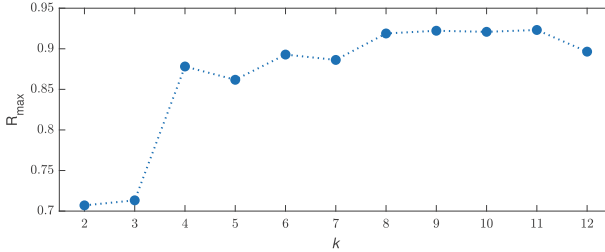


Fig. 6. Correlation coefficients for $k \in [1, 12]$

in the following. By this, it can be extracted in how far the individual clusters resemble each other. Figure 6 shows the maximum correlation coefficient R_{\max} for two individual cluster centers with respect to the number of clusters. R_{\max} slightly increases from $k = 2$ to $k = 3$, and increases significantly for $k = 4$ and reaches a local maximum of about 88%. For larger values of k only a small increase is visible. Hence $k = 3$ is chosen for further examinations to ensure fundamentally different clusters with minimum resemblance.

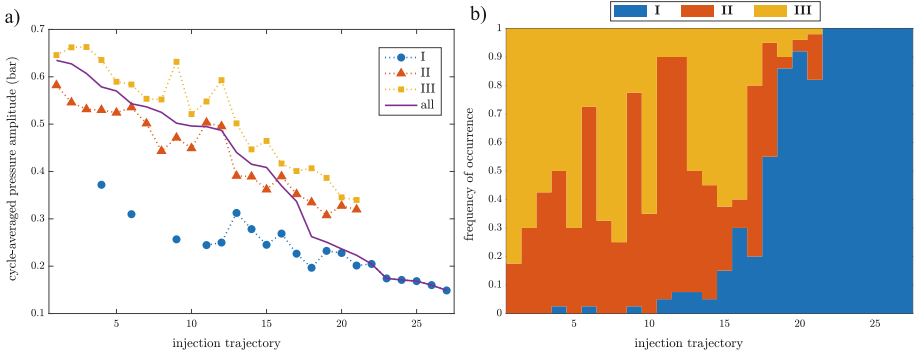


Fig. 7. Result of the k -means algorithm for $k = 3$ for all considered injection trajectories. The injection trajectories are sorted by the cycle-averaged pressure amplitude.

To evaluate the effect of the applied injection trajectory on the probability to observe a specific ignition mode, the frequency of occurrence of the ignition cluster is examined for each injected fuel profile. The applied injection trajectories are sorted with respect to the cycle-averaged maximum pressure amplitude, which is visualized in Fig. 7a (purple line). The amplitude varies from 0.65 bar down to 0.15 bar for the injection trajectories 1 to 27, respectively. It can clearly be seen that pressure signals from clusters **II** and **III** are generally correlated to larger pressure amplitudes. Cluster **I** evokes only small pressure amplitudes compared. At intermediate pressure levels cluster **I** occurs sporadically and is non-existent at high pressures. The opposite applies to clusters **II** and **III**. The frequency of occurrence of each respective cluster for the applied injection trajectory is shown in Fig. 7b. Clusters **II** and **III** appear frequently at injection trajectories that are associated with large pressure amplitudes. For trajectories that are linked to low pressure levels, cluster **III** is predominant. Overall, the data reveals that the frequency of occurrence of the identified clusters can be shifted by the applied injection trajectory, which ultimately causes a variation in the cycle-averaged pressure amplitude.

3.2 Clustering the Fuel Concentration Profiles

To systematically investigate the dependence between the injected fuel profile and the combustion process, the fuel distribution inside the combustor prior to the first detected pressure rise is assessed numerically by applying the previously introduced one-dimensional simulation tool. The obtained axial distributions in fuel concentration are then categorized by k -means clustering. Figure 8 shows the respective fuel clusters obtained for $k = 4$. The gray lines denote the fuel profile, that are assigned to the respective cluster, while the red line represent the cluster centers. Each cluster represents a unique shape of the fuel concentration distribution inside the combustor before the onset of ignition. The fuel clusters

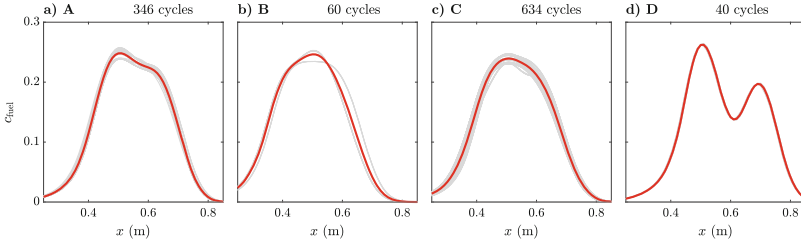


Fig. 8. Result of the k -means algorithm for $k = 4$.

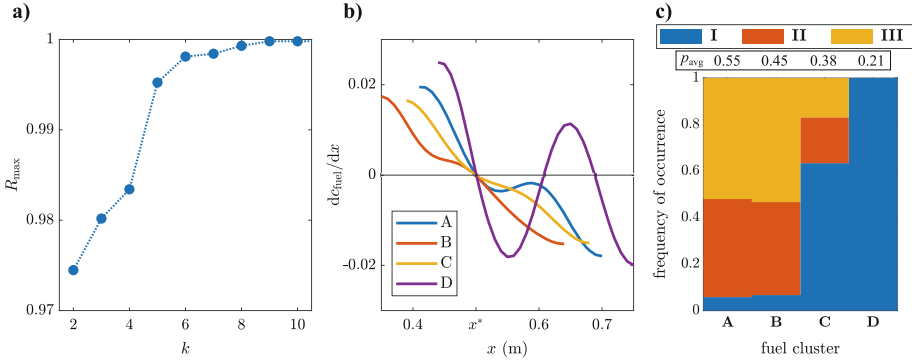


Fig. 9. Frequency of occurrence of ignition patterns with respect to the fuel clusters.

A–D are again sorted with regard to the average pressure rise in the associated combustion cycles.

The maximum correlation coefficient between two clusters R_{\max} is determined and visualized in Fig. 9a to identify a reasonable number of k clusters. In general, an increasing k leads to a higher value of R_{\max} . However, the largest increase is visible from $k = 4$ to $k = 5$. To ensure the identification of fundamentally different injection profiles with reasonably low resemblance, $k = 4$ is considered in the following. This number was chosen as it allows for distinguishing the main features of the fuel profiles, while ensuring a considerable difference between each pair of fuel profile clusters, as visible in Fig. 8. In Fig. 9b, the gradient in fuel distribution for each fuel cluster is visualized. Analogous to the fuel concentration profiles in Fig. 8, the maximum fuel concentration is aligned to $x^* = 0.5$ m, resulting in a zero value for the gradients of all graphs at this position in Fig. 9b. Assuming constant temperature, the ignition event is expected to occur at the axial position of the maximum fuel concentration. According to the observations from Zel'dovich [11], the resulting gradient in mixture reactivity close to this point is decisive for the formation of a certain ignition mode. For fuel cluster **A**, a nearly constant negative gradient is observed for $x > x^*$. In a reasonably large number of cycles, this presumably leads to the formation of a supersonic autoignition front or multiple simultaneous autoignition kernels, both

resulting in a pressure signal associated to the ignition cluster **III**, as shown in Fig. 9c. Similar considerations can be formulated for fuel cluster **B**. Here, a nearly constant positive gradient is observed for $x < x^*$ over a reasonable length. For fuel cluster **C**, the absolute value of the gradient in fuel concentration exhibits a steeper increase in both axial direction from x^* when compared to the fuel clusters **A** and **B**. Thus, the formation of an ignition mode associated with cluster **III** is hindered and the ignition cluster **I** is observed more frequently. Fuel cluster **D** is associated with only minor rise in pressure. Here, two fuel concentration peaks are visible with steep gradients next to the associated axial positions. Clearly, this fuel distribution induces the lowest average pressure rise and the ignition cluster can be entirely assigned to cluster **I**. This goes along with previous investigations in [8] and [10], where optical measurements revealed that a fuel concentration distribution similar to cluster **D** leads to the formation of two turbulent flame fronts, which are initiating with a certain time delay. Hence, no aerodynamic confinement is achieved impeding a large rise in pressure.

4 Conclusion

In this work, the effect of fuel stratification on the formation of autoignition modes is analyzed based on pressure measurements. An SEC test rig is used to measure the pressure rise subsequent to the ignition event for various arbitrary fuel profiles. k -means clustering is used to define a number of ignition clusters based on pressure measurements inside the combustor. It was found that the clusters resemble different autoignition modes observed in previous investigations, namely: turbulent deflagration, subsonic autoignition and supersonic autoignition. In addition, a previously developed one-dimensional simulation tool is used to assess the axial distribution in fuel concentration prior to the ignition event based on the applied injection trajectory. The fuel profiles are subsequently clustered likewise and correlated with the respective ignition clusters. The results show that the gradient in the fuel distribution promotes the occurrence of different autoignition modes. In particular, a decrease in fuel concentration along the combustor length was associated with an increased homogeneity while a fuel distribution with two concentration peaks impedes an aerodynamic confinement causing a low rise in pressure. The cycle-averaged pressure amplitude for a given fuel cluster was found to be highly dependent on the frequency of occurrence of the individual ignition clusters. In conclusion, the cycle-to-cycle variation in the pressure amplitude, which has been observed in previous investigations, can be attributed to the formation of different autoignition modes. The results reveal that the gradient in fuel concentration close to the position of the first ignition greatly impacts the predominant autoignition mode. Based on the findings obtained with regard to the gradient in fuel concentration a more robust control algorithm can be implemented.

Acknowledgment. The authors gratefully acknowledge support by the Deutsche Forschungsgemeinschaft (DFG) as part of Collaborative Research Center SFB 1029

“Substantial efficiency increase in gas turbines through direct use of coupled unsteady combustion” on projects A03. Special thanks go out to Andy Göhrs and Thorsten Dessin for their technical support.

References

1. Berndt, P., Klein, R., Paschereit, C.O.: A kinetics model for the shockless explosion combustion. In: *Turbo Expo: Power for Land, Sea, and Air*, vol. 49767, p. V04BT04A034. American Society of Mechanical Engineers (2016)
2. Bobusch, B.C., Berndt, P., Paschereit, C.O., Klein, R.: Shockless explosion combustion: an innovative way of efficient constant volume combustion in gas turbines. *Combust. Sci. Technol.* **186**(10–11), 1680–1689 (2014)
3. Burke, U., et al.: An ignition delay and kinetic modeling study of methane, dimethyl ether, and their mixtures at high pressures. *Combust. Flame* **162**(2), 315–330 (2015)
4. Dai, P., Qi, C., Chen, Z.: Effects of initial temperature on autoignition and detonation development in dimethyl ether/air mixtures with temperature gradient. *Proce. Combust. Inst.* **36**(3), 3643–3650 (2017)
5. Gu, X.J., Emerson, D.R., Bradley, D.: Modes of reaction front propagation from hot spots. *Combust. Flame* **133**(1–2), 63–74 (2003)
6. Reichel, T., Schäpel, J.S., Bobusch, B.C., Klein, R., King, R., Paschereit, C.O.: Shockless explosion combustion: experimental investigation of a new approximate constant volume combustion process. *J. Eng. Gas Turb. Power* **139**(2), 021504 (2017)
7. Warnatz, J., Maas, U., Dibble, R.: *Combustion*. Springer, Berlin (2006). <https://doi.org/10.1007/978-3-540-45363-5>
8. Yücel, F.C., Habicht, F., Bohon, M., Paschereit, C.O.: Autoignition in stratified mixtures for pressure gain combustion. *Proc. Combust. Inst.* **38**(3), 3815–3823 (2021)
9. Yücel, F.C., Habicht, F., Jaeschke, A., Lückoff, F., Oberleithner, K., Paschereit, C.O.: Investigation of the fuel distribution in a shockless explosion combustor. In: *Turbo Expo: Power for Land, Sea, and Air*, vol. 84133, p. V04BT04A058. American Society of Mechanical Engineers (2020)
10. Yücel, F.C., Habicht, F., Arnold, F., King, R., Bohon, M., Paschereit, C.O.: Controlled autoignition in stratified mixtures. *Combust. Flame* **232**, 111533 (2021)
11. Zeldovich, Y.B.: Regime classification of an exothermic reaction with nonuniform initial conditions. *Combust. Flame* **39**(2), 211–214 (1980)